



APPLICATION OF A MODIFIED VLASOV MODEL TO EARTHQUAKE ANALYSIS OF PLATES RESTING ON ELASTIC FOUNDATIONS

Y. AYVAZ, A. DALOĞLU AND A. DOĞANGÜN

Department of Civil Engineering, Karadeniz Technical University, 61080 Trabzon, Turkey

(Received 3 June 1997, and in final form 10 November 1997)

An application is presented of a modified Vlasov model to earthquake analysis of plates resting on an elastic foundation. The effects of the subsoil depth, the plate dimensions and their ratios on the dynamic response are investigated. The method of finite elements is used for spatial integration and the Newmark- β method is used for time integration. A number of graphs are presented to show the effects of plate dimensions and the subsoil depth on the dynamic out-of-plane responses of plates on elastic foundations. Numerical examples associated with the applicability of the model to earthquake analysis of plates resting on elastic foundations are given.

© 1998 Academic Press Limited

1. INTRODUCTION

The concept of plates resting on elastic foundations is extensively used by structural and geotechnical engineers for static and dynamic analyses and for design of many practical soil–structure interaction problems such as floor slabs of multistory buildings, highways and airfield pavements. Developing a more realistic mathematical model for this complex soil–structure interaction problem is essential to provide an accurate analysis of the soil–structure system for safe and economical design. The well-known Winkler foundation model has been widely used to analyze beams and plates resting on elastic foundations because of its simplicity. Static and dynamic analyses of beams on elastic foundation using the Winkler model have been performed by many authors [1–4]. Another simple model, known as the Pasternak model, is obtained by connecting the top of the Winkler springs with a shear layer. This model is also called the two-parameter foundation model and has been used for dynamic analysis of beams on elastic foundation by several researchers [5–7]. Vlasov [8] developed a three-parameter model for beams and plates on elastic foundations by introducing an arbitrary parameter γ , including the effect of the shear strain energy in the soil and the subsequent shear forces on the beam and plate edges. An iterative technique using the modified Vlasov model has been performed for static analysis of plates on elastic foundation [9, 10]. The same procedure was also used for dynamic analysis of beams on elastic foundations [11, 12]. However, no studies have been found for the dynamic analysis of plates resting on elastic foundations using the modified Vlasov model.

The aim in this paper is to analyze the dynamic behavior of foundation plates subjected to earthquake loading using the modified Vlasov model. The finite element method is used for spatial integration and the Newmark- β method is used for time integration. Stiffness matrices and the mass matrix are obtained by using the so-called MZC rectangle finite elements [13, 14]. An iterative solution technique depending upon the parameter γ is applied to investigate the effects of the subsoil depth, plate dimensions and their ratios on

the response of rectangular plates on elastic foundations subjected to earthquake loading. Numerical examples are given to show the performance and effectiveness of the proposed finite element approach.

2. MATHEMATICAL MODEL

The governing equation for a flexural plate subjected to an earthquake excitation with no damping can be given as

$$[\mathbf{M}]\{\ddot{\mathbf{w}}\} + [\mathbf{K}]\{\mathbf{w}\} = -[\mathbf{M}]\{\ddot{\mathbf{u}}_g\}, \quad (1)$$

where $[\mathbf{K}]$ and $[\mathbf{M}]$ are the stiffness matrix and the mass matrix of the plate-soil system, w and \ddot{w} are the lateral displacement and the acceleration of the plate, and \ddot{u}_g is the vertical component of the earthquake acceleration.

2.1. TOTAL STRAIN ENERGY OF PLATE-SOIL SYSTEM

An expanded form of the total strain energy in the soil-structure system (see Figure 1) may be written as

$$\Pi = \Pi_p + \Pi_s + V, \quad (2a)$$

where Π_p is the strain energy in the plate,

$$\Pi_p = \frac{1}{2} \int_{\Omega} \left(\frac{\partial^2 w}{\partial x^2}, \frac{\partial^2 w}{\partial y^2}, 2 \frac{\partial^2 w}{\partial x \partial y} \right) [\mathbf{D}] \left(\frac{\partial^2 w}{\partial x^2}, \frac{\partial^2 w}{\partial y^2}, 2 \frac{\partial^2 w}{\partial x \partial y} \right)^T dx dy, \quad (2b)$$

Π_s is the strain energy stored in the soil,

$$\Pi_s = \frac{1}{2} \int_0^H \int_{-\infty}^{\infty} \int_{-\infty}^{\infty} \sigma_{ij} \epsilon_{ij} dx dy dz \quad (2c)$$

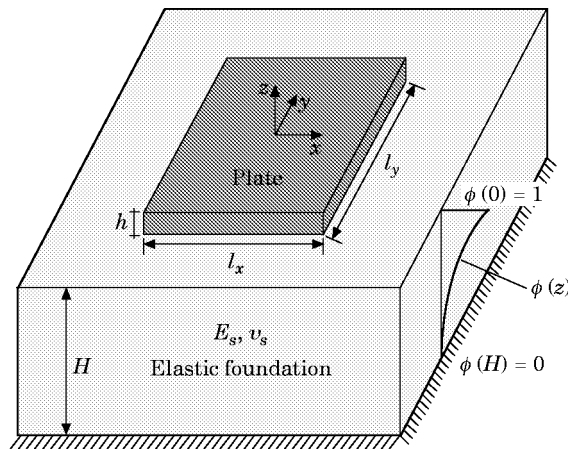


Figure 1. A sample plate on an elastic foundation.

and V is the potential energy of the earthquake loading,

$$V = - \int_{\Omega} \bar{q} w \, dx \, dy. \quad (2d)$$

In these equations, w is the displacement of the plate in the vertical z direction, D is the flexural rigidity of the plate [10], H is the depth of the soil continuum, x, y, z are the co-ordinate axes as shown in Figure 1, Ω is the domain of the plate, and \bar{q} denotes

$$-[\mathbf{M}]\{\ddot{\mathbf{u}}_g\}.$$

According to the Kirchhoff theory for thin plates, the constitutive relation for the soil medium are

$$\bar{\sigma}_{ij} = \lambda \delta_{ij} \bar{\epsilon}_{kk} + 2G \bar{\epsilon}_{ij} \quad (3)$$

where λ and G are the Lamé parameters [15] for a homogeneous and isotropic soil medium, δ_{ij} is the Kronecker delta, and $\sigma_{ij}, \epsilon_{ij}$ are the stress and strain tensors in the soil continuum, respectively.

To simplify the model, the displacements in the x and y directions may be assumed to be equal to zero. Further it is assumed that

$$\bar{w}(x, y, z) = w(x, y)\phi(z), \quad (4)$$

so that $\bar{w}(x, y, 0)$ becomes the vertical displacement of the surface of the soil and $\phi(z)$ is a mode shape function defining the variation of $w(x, y, z)$ in the z direction.

Using variational principles and minimizing the total potential energy of equation (2a) by taking variations in w and ϕ yield [16] the following field equations. The field equation in the domain of the plate, Ω , is

$$D \nabla^4 w - 2t \nabla^2 w + kw = \bar{q}. \quad (5a)$$

Outside the plate domain, the field equation is

$$-2t \nabla^2 w + kw = 0, \quad (5b)$$

and the field equation in the domain of the soil for $0 \leq z \leq H$ with the boundary conditions $\phi(0) = 1$ and $\phi(H) = 0$ is

$$-m \, d^2\phi/dz^2 + n\phi = 0. \quad (5c)$$

In these equations

$$k = \int_0^H \bar{E} \left(\frac{d\phi}{dz} \right)^2 dz, \quad 2t = \int_0^H G_s \phi^2 dz, \quad (6a, b)$$

$$m = \int_{-\infty}^{\infty} \int_{-\infty}^{\infty} \bar{E} w^2 \, dx \, dy, \quad n = \int_{-\infty}^{\infty} \int_{-\infty}^{\infty} G_s (\nabla w)^2 \, dx \, dy. \quad (6c, d)$$

Here G_s is the shear modulus of the subsoil and

$$\bar{E} = E_s(1 - \nu_s)/(1 + \nu_s)(1 - 2\nu_s). \quad (7)$$

where E_s and ν_s are the modulus of elasticity and Poisson's ratio of the soil, respectively.

The solution of equation (5c) for the given boundary conditions yields

$$\phi(z) = \sinh \gamma(1 - z/H)/\sinh \gamma, \quad (8)$$

where $\gamma/H = -n/m$ represents the variation of the deformation of the soil along the z -axis [10, 16].

Equation (5b) has to be solved in the domain outside the plate with $z = 0$. Vlasov and Leont'ev [8] assumed an approximate solution for the displacement function $w(x, y)$ by dividing the domain outside the plate into eight regions, see references [10, 16] for more explanation.

2.2. STIFFNESS MATRICES

As mentioned before, the so-called MZC rectangle finite element is used in this study. Nodal displacements at each node are

$$w_i, \partial w_i/\partial y, -\partial w_i/\partial x, \quad i = 1, 2, 3, 4, \quad (9a)$$

and the displacement function is

$$w = [\mathbf{N}]\{\mathbf{w}_e\}, \quad (9b)$$

where $\{\mathbf{w}_e\}$ is the nodal displacement vector containing all 12 components of the type shown in equation (9a).

The matrix $[\mathbf{N}]$ contains the displacement shape functions [13, 14]. The stiffness matrices of the plate and the soil can be derived by substituting equation (9b) into equation (2a).

By using the standard procedure in the finite element methodology for the assemblage of elements, the global stiffness matrix is constructed as a half-banded matrix,

$$[\mathbf{K}] = \sum_{i=1}^n ([\mathbf{k}_p] + [\mathbf{k}_k] + [\mathbf{k}_t]), \quad (10a)$$

where n is the total number of the plate finite elements, and $[\mathbf{k}_p]$ is the conventional element stiffness matrix of the plate [13, 14]. The stiffness matrix for the axial strain effect in the soil, $[\mathbf{k}_k]$, is obtained by minimizing the total energy with respect to each component of the displacement vector [10], and may be written as

$$[\mathbf{k}_k] = kab \int_{-1}^1 \int_{-1}^1 [N]^T [N] d\xi d\eta, \quad (10b)$$

in which a and b are the plate dimensions, and ξ and η are natural co-ordinates. $[\mathbf{k}_t]$ is the stiffness matrix which accounts for the shear effect in the soil, expressed as

$$[\mathbf{k}_t] = 2tab \int_{-1}^1 \int_{-1}^1 \left(\frac{1}{a^2} \begin{bmatrix} \partial N \\ \partial \xi \end{bmatrix}^T \begin{bmatrix} \partial N \\ \partial \xi \end{bmatrix} + \frac{1}{b^2} \begin{bmatrix} \partial N \\ \partial \eta \end{bmatrix}^T \begin{bmatrix} \partial N \\ \partial \eta \end{bmatrix} \right) d\xi d\eta. \quad (10c)$$

The matrices $[\mathbf{k}_k]$ and $[\mathbf{k}_t]$ are not presented here since they will take excessive space, so for more information about these matrices, see reference [10].

Equivalent nodal loads $\{\mathbf{F}\}$ can be computed as

$$\{\mathbf{F}\} = \int_{\Omega} N_i^T \bar{q} dx. \quad (11)$$

2.3. MASS MATRIX

The dynamics of elastic structures is based on Hamilton's variational principle with the kinetic energy of

$$\Pi_k = \frac{1}{2} \int_{\Omega} \dot{\mathbf{w}}^T \mu \dot{\mathbf{w}} \, d\Omega, \quad (12a)$$

where w represents the vector of generalized displacement components relevant to inertial forces, the dot denotes the partial derivative with respect to time t , and μ is the mass density matrix of the form

$$\mu = \begin{bmatrix} m_1 & 0 & 0 \\ 0 & m_2 & 0 \\ 0 & 0 & m_3 \end{bmatrix}, \quad (12b)$$

where $m_1 = \rho_p h + \frac{1}{3}(\rho_s H)$, $m_2 = m_3 = \frac{1}{12}(\rho_p h^3)$, h is the thickness of the plate, and ρ_p and ρ_s are the mass densities of the plate and the soil, respectively [17].

Then the formula for the consistent mass matrix of the plate on the elastic foundation may be written as

$$M = \int_{\Omega} N_i^T \mu N_i \, d\Omega. \quad (12c)$$

In view of equation (9b), the following equation can be written for each finite element:

$$N_i = [N, dN/dy, dN/dx]. \quad (12d)$$

The consistent mass matrix of the plate-soil system can be evaluated by substituting equation (12d) into equation (12c) and integrating it over the domain. It is a symmetric 12×12 matrix, and its upper triangle is given in the Appendix for a rectangular finite element with the dimensions of $2a \times 2b$.

It should be noted that, in this study, the Newmark- β method is used for the time integration of equation (1) by using the average acceleration method [18].

4. NUMERICAL EXAMPLES

4.1. THE SOLUTION TECHNIQUE

A computer program is coded in FORTRAN for the dynamic analysis of the rectangular plate on an elastic foundation. The solution technique is an iterative process. Displacement computations are dependent upon the value of the γ parameter which is initially set equal to 1.0 when the time is equal to zero. The mode shape ϕ is calculated and used for the computation of the values of the modulus of the subgrade reaction, k , and the soil shear parameter, $2t$. Then these values are used to construct the coefficient matrices of the plate-soil system and to calculate the displacement at discrete points of the finite element mesh. Next the value of γ is calculated, and the process is repeated for the new value of γ until the difference between the two successive values of γ is less than a small prescribed value, say equal to 0.001. The procedure described above is repeated for each time increment. The final value of γ at each time increment is taken to be the initial value of γ for the next time increment.

4.2. DATA FOR NUMERICAL EXAMPLES

In the light of the results given in reference [11, 19], the depths H of the subsoil are taken to be 5 m, 10 m, and 15 m. The aspect ratio, l_y/l_x , of the plate are taken to be 1, 1.5, and 2.0. The ratios, H/l_y , are taken as 0.25, 0.50, 0.75, and 1.0 for each subsoil depth considered. The shorter length, l_x , of the plate is kept constant at 10 m. The mass densities of the plate and the subsoil are taken to be 2500 kg/m³ and 1700 kg/m³, respectively.

In order to obtain the response of each plate, the first 10 s of the vertical component of the March 13, 1992 Erzincan earthquake in Turkey is used since the peak value of the record occurred in this range [20]. Also, after the tenth second, it is seen that the responses of the plate remained almost constant since no damping is considered in the study.

For the sake of accuracy in the results, rather than starting with a set of a finite element mesh size and time increment, the mesh size and time increment required to obtain the desired accuracy were determined before presenting any results. This analysis was performed separately for the mesh size and time increment. It was concluded that the results have acceptable error when equally spaced 10×10 elements are used for a $10 \text{ m} \times 10 \text{ m}$ plate if the 0.01 s time increment is used. Lengths of the elements in the x and y directions are kept constant for different l_y/l_x ratios.

4.3. RESULTS

The purpose of this study was to calculate the time histories of the displacements at different points on the plates considered for different subsoil depths and aspect ratios, but presentation of all of the time histories would take up excessive space. Hence, only the maximum displacements for different aspect ratios and subsoil depths are presented after two time histories are given. This simplification of presenting only the maximum responses is supported by the fact that the maximum values of these quantities are the most important ones for design. These results are presented in graphical, rather than in tabular form.

The time histories of the center displacements of the plates for $l_y = 10 \text{ m}$ and 20 m when $H = 5 \text{ m}$ are given in Figure 2 for a constant l_x value of 10 m. The center displacements of $10 \text{ m} \times 10 \text{ m}$ and $10 \text{ m} \times 20 \text{ m}$ plates for $H = 5 \text{ m}$ reached their absolute maximum values of 9 mm at 9.05 s, and of 20.3 mm at 7.70 s as can be seen from Figures 2(a) and 2(b). The maximum displacement of $10 \text{ m} \times 20 \text{ m}$ plate is larger than that of the $10 \text{ m} \times 10 \text{ m}$ plate as expected.

Figures (2a, b) indicate that the time histories of the center displacements of the plates are different even with the same subsoil depth, as the dynamic characteristics of the plate-soil system affect the responses, and that the periods of the center displacements are becoming larger with increasing subsoil depth for a fixed aspect ratio and with increasing aspect ratio for a fixed subsoil depth. This is expected since the system becomes more flexible when the aspect ratio of the plate and/or the subsoil depth increases.

The maximum displacements of the plate are given in Figures 3 and 4 for different H values, aspect ratios, and H/l_y ratios. In these figures, the bottom part shows the upward displacement, and the top part shows the downward displacements. These figures also indicate that the maximum displacements do not vary in a smooth simple way as in the case of static displacements. This behavior is due to sensitivity of the response to small changes in the dynamic characteristics of the plates resting on elastic foundation.

Several general trends illustrated in Figures 3 and 4 are instructive, despite the somewhat irregular patterns in the curves. The trends seen from these figures are as follows.

The maximum displacement increases with an increasing value of H for any value of the aspect ratio, l_y/l_x .

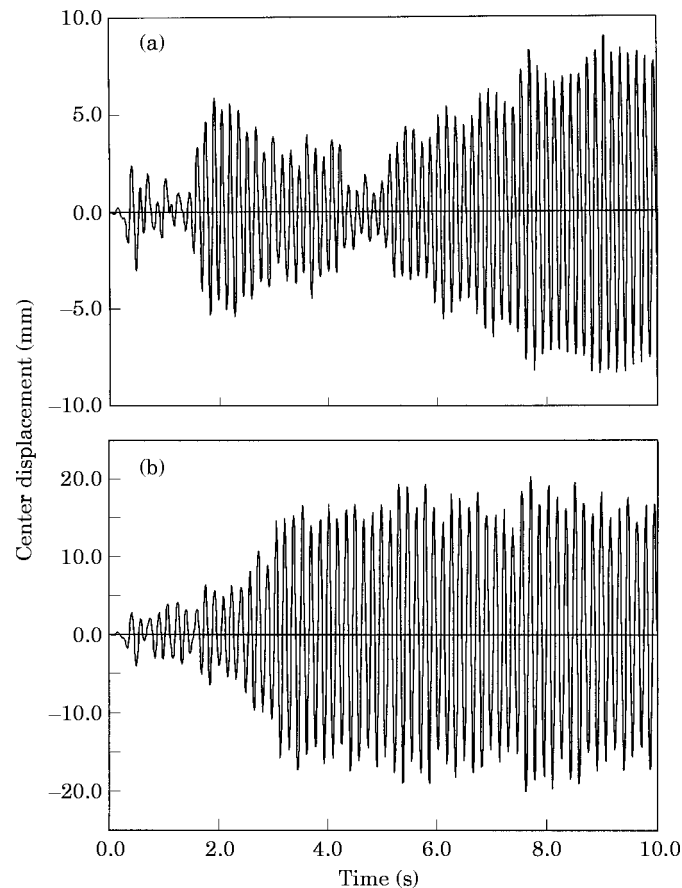


Figure 2. The time history of the center displacement of the plate (a) for $H = 5$ m and $l_y = 10$ m; (b) for $H = 5$ m and $l_y = 20$ m.

The maximum displacement does not always decrease or increase with increasing values of l_y/l_x for any values of the subsoil depth H . This irregular pattern is due to sensitivity of the response to small changes in the period of the system.

The maximum displacement is more sensitive to the changes in the subsoil depth than the changes in the aspect ratio.

The maximum displacement generally decreases as H/l_y ratios increase for any values of H . The exceptions to this trend in Figure 4, especially for $H = 15$ m, are caused by dramatic changes in the dynamic amplification factor as peaks and valleys are traversed due to changes in the period of the system, as in the case of a beam resting on an elastic foundation [11] and of a plate [21].

The maximum displacement always increases with increasing subsoil depth for any values of H/l_y ratios.

The deflected shapes of the plates on an elastic foundation for $l_y/l_x = 1$ and 2 when $H = 15$ m for the time at which the maximum displacement occurs are given in Figure 5. The deflected shapes of the other plates considered are not presented since they are similar to the ones given here.

A plate on an elastic foundation with a larger subsoil depth and aspect ratio becomes more flexible and thus less resistant to the load, so that this system will have a larger displacement in a static sense, but this is not always satisfied, especially for $H = 15$ m,

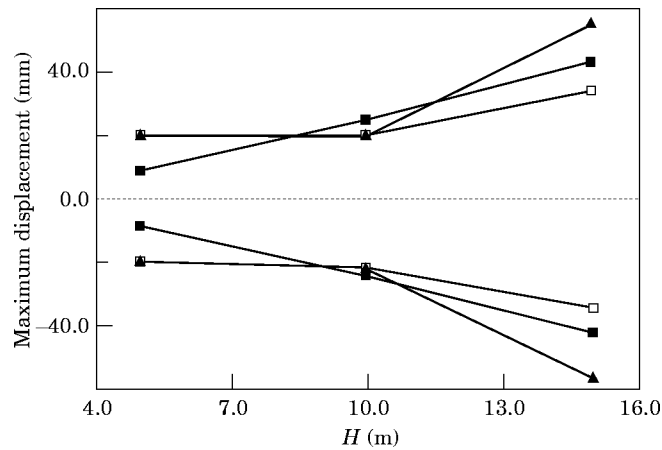


Figure 3. The maximum displacement of the plate for different subsoil depths and aspect ratios. l_y/l_x values: \blacksquare -, 1.0; \square -, 1.5; \blacktriangle -, 2.0.

because the maximum displacement of the dynamic system changes, depending on the dynamic characteristics of the system.

In conclusion, it may be said that the maximum displacements of a plate resting on an elastic foundation sometimes tend to be sensitive to small changes in the dynamic characteristics, such as the period, as the subsoil depth and/or aspect ratio are changed.

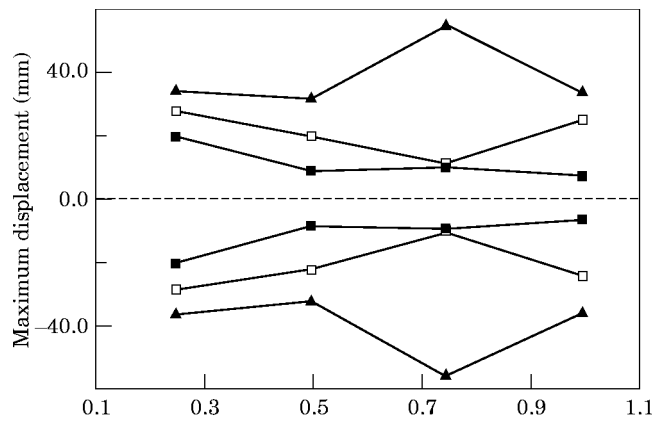


Figure 4. The maximum displacement of the plate for different H/l ratios and subsoil depths. H values (m): \blacksquare -, 5; \square -, 10; \blacktriangle -, 15.

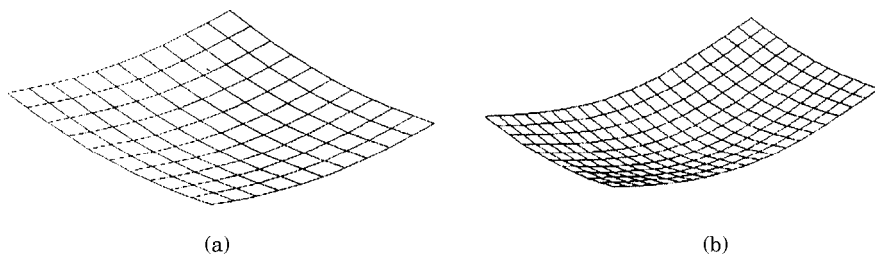


Figure 5. The deflected shape of the plate for different aspect ratios ($H = 15$ m). l_y/l_x values: (a) 1, (b) 2.

TABLE 1
The maximum and minimum γ values for different subsoil depths and aspect ratios

H (m)	l_y/l_x	γ_{min}	γ_{max}
5	1.00	0.79	2.37
	1.50	0.70	1.79
	2.00	0.66	1.36
10	1.00	1.24	4.49
	1.33	1.13	3.68
	1.50	1.09	3.15
	2.00	1.01	2.24
15	4.00	0.90	2.11
	1.00	1.61	4.17
	1.50	1.41	4.23
	2.00	1.30	3.16
	3.00	1.19	3.81
	6.00	1.08	2.14

Despite their irregularities, the curves show trends that can be readily understood, and that can be utilized in choosing the aspect ratio, depending on the subsoil depth when it is known.

It should be noted that the results obtained by using the modified Vlasov model are not compared with the results of Winkler model, which is simpler, because the stiffness parameter, k , which has a constant value in the Winkler model at all time increments, takes different values in the modified Vlasov model at each time increment.

The maximum and minimum values of the parameter γ obtained at each run for different subsoil depths and aspect ratios are presented in Table 1. As seen from this table, the values of γ increase with increasing subsoil depth for any values of the aspect ratios, except that the maximum value of γ decreases when H is increased from 10 m to 15 m for $l_y/l_x = 1$. In addition, the values of γ decrease with increasing aspect ratio for a fixed subsoil depth, except that the maximum value of γ increases when l_y/l_x is increased from 1.0 to 1.5 for $H = 15$ m. This result complies with the results obtained previously [11, 19]. As the value of γ increases, the ϕ function of equation (8) represents a rapidly dissipating displacement, which is typical for large values of H . When the value of γ approaches zero, the function ϕ yields a linear variation in displacements from top to bottom [19]. It should be noted that most values of γ obtained at each time increment are close to the minimum γ for all values of the subsoil depths.

For a plate resting on an elastic foundation subjected to the vertical component of an earthquake excitation, it is somewhat difficult to interpret the effects of the subsoil depth and the aspect ratio on the response, because both the frequency content of the earthquake excitation and the exact natural frequency of the particular plate can make a difference to its response. The curves presented herein can help the designer to anticipate the effects of the subsoil depth and the aspect ratio on the earthquake response of a plate resting on an elastic foundation.

5. CONCLUSIONS

The modified Vlasov model has been applied effectively to the earthquake analysis of plates resting on elastic foundations. Two soil parameters were iteratively calculated

depending on the parameter γ which controls the decay of the stress distribution within the foundation.

The following conclusions can be obtained from the study.

The maximum displacement increases with an increasing value of H for any values of the aspect ratio.

The maximum displacement generally decreases as the H/l_y ratio increases for any values of H .

The maximum displacement increases with increasing subsoil depth for any values of the H/l_y ratio.

In general, the maximum displacement is more sensitive to the changes in the subsoil depth than to the changes in the aspect ratio.

REFERENCES

1. M. HETENYI 1961 *Beams on Elastic Foundation*. Ann Arbor: University of Michigan Press.
2. Z. DING 1993 *Computers and Structures* **47**, 83–90. A general solution to vibrations of beams on variable Winkler elastic foundation.
3. M. A. DE ROSA 1989 *Earthquake Engineering and Structural Dynamics* **18**, 341–349. Stability and dynamics of beams on Winkler elastic foundation.
4. M. EISENBERGER, D. Z. YANKEKEVSKY and J. CLASTORNIK 1986 *Computers and Structures* **24**, 135–140. Stability of beams on elastic foundations.
5. C. FRANCIOSI and A. MASI *Computers and Structures* **47**, 419–426. Free vibrations of foundation beams on two-parameter elastic soil.
6. M. A. DE ROSA 1993 *Computers and Structures* **49**, 341–349. Stability and dynamic analysis of two-parameter foundation beams.
7. T. YOKOYAMA 1996 *Computers and Structures* **61**, 995–1007. Vibration analysis of Timoshenko beam-columns on two-parameter elastic foundations.
8. V. Z. VLASOV and U. N. LEONTIEV 1996 *Beams, Plates and Shells on Elastic Foundations*. Jerusalem: Israel Program for Scientific Translations.
9. W. T. STRAUGHAN 1990 *Ph.D. Thesis, The Graduate School of Texas Tech University, Lubbock, Texas*. Analysis of plates on elastic foundations.
10. A. TURHAN 1992 *Ph.D. Thesis, The Graduate School of Texas Tech University, Lubbock, Texas*. A consistent Vlasov model for analysis of plates on elastic foundations using the finite element method.
11. Y. AYVAZ and A. DALOĞLU 1997 *Journal of Sound and Vibration* **200**, 315–325. Earthquake analysis of beams resting on elastic foundations by using a modified Vlasov model.
12. A. DALOĞLU and Y. AYVAZ 1996 *Proceeding of the Second International Conference in Civil Engineering on Computer Applications, Research and Practice* **3**, 901–907. Vibration analysis of beams on elastic foundation using modified Vlasov model.
13. O. C. ZIENKIEWICZ 1977 *The Finite Element Method*. London: McGraw-Hill Ltd. (third edition).
14. W. WEAVER and P. R. JOHNSTON 1984 *Finite Element for Structural Analysis*. Englewood Cliffs, NJ: Prentice-Hall.
15. S. P. TIMOSHENKO and S. WOINOWSKY-KRIEGER 1965 *Theory of Plates and Shells*. New York: McGraw-Hill.
16. C. V. G. VALLABHAN, W. T. STRAUGHAN and Y. C. DAS 1991 *Journal of Engineering Mechanics* **117**, 2830–2844. A refined model for analysis of plates on elastic foundations.
17. V. KOLAR and I. NEMEC 1989 *Modelling of Soil-Structure Interaction*. Amsterdam: Elsevier.
18. J. L. HUMAR 1990 *Dynamics of Structures*. Englewood Cliffs, NJ: Prentice-Hall.
19. C. V. G. VALLABHAN and Y. C. DAS 1991 *International Journal of Solids and Structures* **27**, 629–637. A refined model for beams on elastic foundations.
20. A. DURMUS 1993 *Advances in Civil Engineering, The First Technical Congress* **1**, 93–101. Evaluation of the behavior of reinforced concrete structures in Erzincan subjected to the March 13, 1992 Erzincan earthquake (in Turkish).
21. Y. AYVAZ and A. DURMUS 1995 *Journal of Sound and Vibration* **187**, 531–539. Earthquake analysis of simply supported reinforced concrete slabs.

APPENDIX: MASS MATRIX

$$\begin{aligned}
m_{1,1} &= \frac{1727}{3150}m_1 + \frac{46}{105}(m_2 + m_3), & m_{1,2} &= \frac{461}{3150}m_1b + \frac{1}{15}m_2b + \frac{11}{105}m_3b, \\
m_{1,3} &= -\frac{461}{3150}m_1a - \frac{11}{105}m_2a - \frac{1}{15}m_3a, & m_{1,4} &= \frac{613}{3150}m_1 + \frac{17}{105}m_2 - \frac{46}{105}m_3, \\
m_{1,5} &= \frac{199}{3150}m_1b + \frac{1}{30}m_2b - \frac{11}{105}m_3b, & m_{1,6} &= +\frac{137}{1575}m_1a + \frac{13}{210}m_2a - \frac{1}{15}m_3a, \\
m_{1,7} &= \frac{197}{3150}m_1 - \frac{17}{105}(m_2 + m_3), & m_{1,8} &= -\frac{58}{1575}m_1b + \frac{1}{30}m_2b + \frac{13}{210}m_3b, \\
m_{1,9} &= \frac{58}{1575}m_1a - \frac{13}{210}m_2a - \frac{1}{30}m_3a, & m_{1,10} &= \frac{613}{3150}m_1 - \frac{46}{105}m_2 + \frac{17}{105}m_3, \\
m_{1,11} &= -\frac{137}{1575}m_1b + \frac{1}{15}m_2b - \frac{13}{210}m_3b, & m_{1,12} &= -\frac{199}{3150}m_1a - \frac{11}{105}m_2a - \frac{1}{30}m_3a, \\
m_{2,2} &= \frac{16}{315}m_1b^2 + \frac{8}{45}m_2b^2 + \frac{4}{105}m_3b^2, & m_{2,3} &= -\frac{1}{25}m_1ba, & m_{2,4} &= m_{1,5} \\
m_{2,5} &= \frac{8}{315}m_1b^2 + \frac{4}{45}m_2b^2 - \frac{4}{105}m_3b^2, & m_{2,6} &= \frac{2}{75}m_1ba, \\
m_{2,7} &= \frac{58}{1575}m_1b - \frac{1}{30}m_2b - \frac{13}{210}m_3b, & m_{2,8} &= -\frac{2}{105}m_1b^2 - \frac{1}{45}m_2b^2 + \frac{1}{35}m_3b^2, \\
m_{2,9} &= \frac{4}{225}m_1ba, & m_{2,10} &= -m_{1,11}, & m_{2,11} &= -\frac{4}{105}m_1b^2 - \frac{2}{45}m_2b^2 - \frac{1}{35}m_3b^2, \\
m_{2,12} &= -m_{2,6}, & m_{3,3} &= \frac{16}{315}m_1a^2 + \frac{4}{105}m_2a^2 + \frac{8}{45}m_3a^2, & m_{3,4} &= -m_{1,6}, \\
m_{3,5} &= -m_{2,6}, & m_{3,6} &= -\frac{4}{105}m_1a^2 - \frac{1}{35}m_2a^2 - \frac{2}{45}m_3a^2, & m_{3,7} &= -m_{1,9}, & m_{3,8} &= m_{2,9}, \\
m_{3,9} &= -\frac{2}{105}m_1a^2 + \frac{1}{35}m_2a^2 - \frac{1}{45}m_3a^2, & m_{3,10} &= -\frac{199}{3150}m_1a + \frac{11}{105}m_2a - \frac{1}{30}m_3a, \\
m_{3,11} &= m_{2,6}, & m_{3,12} &= \frac{8}{315}m_1a^2 - \frac{4}{105}m_2a^2 + \frac{4}{45}m_3a^2, & m_{4,4} &= m_{1,1}, & m_{4,5} &= m_{1,2}, \\
m_{4,6} &= -m_{1,3}, & m_{4,7} &= m_{1,10}, & m_{4,8} &= -m_{2,10}, & m_{4,9} &= -m_{3,10}, & m_{4,10} &= m_{1,7}, \\
m_{4,11} &= m_{2,7}, & m_{4,12} &= m_{3,7}, & m_{5,5} &= m_{2,2}, & m_{5,6} &= -m_{2,3}, & m_{5,7} &= m_{2,10}, \\
m_{5,8} &= m_{2,11}, & m_{5,9} &= -m_{3,5}, & m_{5,10} &= -m_{2,7}, & m_{5,11} &= m_{2,8}, & m_{5,12} &= m_{2,9}, \\
m_{6,6} &= m_{3,3}, & m_{6,7} &= -m_{3,10}, & m_{6,8} &= -m_{2,6}, & m_{6,9} &= m_{3,1}, & m_{6,10} &= m_{1,9}, \\
m_{6,11} &= -m_{2,9}, & m_{6,12} &= m_{3,9}, & m_{7,7} &= m_{1,1}, & m_{7,8} &= -m_{1,2}, & m_{7,9} &= -m_{1,3}, \\
m_{7,10} &= m_{1,4}, & m_{7,11} &= -m_{1,5}, & m_{7,12} &= -m_{1,6}, & m_{8,8} &= m_{2,2}, & m_{8,9} &= m_{2,3}, \\
m_{8,10} &= -m_{1,5}, & m_{8,11} &= m_{2,5}, & m_{8,12} &= m_{2,6}, & m_{9,9} &= m_{3,3}, & m_{9,10} &= m_{1,6}, \\
m_{9,11} &= -m_{2,6}, & m_{9,12} &= m_{3,6}, & m_{10,10} &= m_{1,1}, & m_{10,11} &= -m_{1,2}, & m_{10,12} &= -m_{1,3}, \\
m_{11,11} &= m_{2,2}, & m_{11,12} &= -m_{2,3}, & m_{12,12} &= m_{3,3}.
\end{aligned}$$